**Research Article** **Open Access**

Mario Kubanik, Jason K. Y. Tu, Tilo Söhnel, Michaela Hejl, Michael A. Jakupec, Wolfgang Kandioller, Bernhard K. Keppler, Christian G. Hartinger*

# Expanding on the Structural Diversity of Flavone-Derived Ruthenium$^{II}$($\eta^6$-arene) Anticancer Agents

DOI 10.1515/medr-2015-0001
Received June 30, 2015; accepted August 8, 2015

**Abstract:** 3-Hydroxyflavones belong to the naturally occurring class of flavonoids and have been extensively studied with regard to medicinal application. Moreover, it has been demonstrated that these compounds act as bioactive chelates to the ruthenium(II)–arene moiety. Such organometallic complexes have shown promising anticancer activity against tumor cells via a multitargeting mode of action, interacting with DNA and inhibiting topoisomerase IIα. In this paper, we present the synthesis and characterization of an extended series of 3-hydroxyflavone ligands and their corresponding ruthenium-*p*-cymene complexes to study the impact of substitution pattern as well as of electron-withdrawing and –donating substituents at the flavonol-phenyl group. The ligands and complexes were characterized by elemental analysis, ESI-MS, 1D as well as 2D NMR spectroscopy. The structures of four Ru(η$^6$-*p*-cymene) complexes were determined in solid state by single-crystal X-ray diffraction, and the impact of the substitution pattern with regard to *in vitro* anticancer activity in human cancer cell lines is discussed. Structural differences, calculated octanol-water partition coefficients (clog*P*) of the flavonols and aqueous solubility were used to rationalize the finding that chlorido[3-(oxo-κ*O*)-2-(3,5-dimethoxyphenyl)-chromen-4-onato-κ*O*](η$^6$-*p*-cymene) ruthenium(II) **2b** exhibits the highest cytotoxicity with $IC_{50}$ values in the low μM range in all tested cell lines.

**Keywords:** Bioorganometallic chemistry, Cancer chemotherapy, Flavonols, Ruthenium complexes, X-ray diffraction analysis

## 1 Introduction

Conventional cytotoxic chemotherapeutics effectively kill tumor cells but their low selectivity often results in damage to healthy organs and tissues [1]. Therefore, strategies that improve the specificity of chemotherapies in the human body (e.g. targeted delivery, molecular targeted therapies) maximize the drugs' anticancer activity while they reduce the systemic toxicity to non-tumor tissue. In recent years, such strategies have become popular in the development of cancer chemotherapeutics, including also metal-based drugs. For, example, the established Pt(ammine)$_2$ pharmacophore of cisplatin has been modified to improve the selectivity by using ligands which can specifically bind to certain transporters, enzymes and receptors, or by using platinum(IV) compounds as prodrug [2].

Within the course of developing non-platinum anticancer agents, Ru compounds with different activity profiles have moved into the focus of interest. They were often described as less toxic than platinum complexes, which have been attributed to a higher selectivity for tumor cells. Both more selective delivery, tumor (cell)-dependent activation and targeted activity have been suggested to be responsible for these properties. Promising examples feature ligands such as paullones [3], *N*-heterocyclic carbenes [4], quinones [5] and protein-targeting approaches (e.g. ethacrynic acid [6,7], maleimide [8,9], acetal [10], biotin [11,12] and aldehyde [13]), or resemble biological substrates of kinases [14,15].

We have focused in the last years on developing organometallic compounds based on biologically active

***Corresponding author: Christian Hartinger:** School of Chemical Sciences, University of Auckland, Private Bag 92019, Auckland 1142, New Zealand, E-mail: c.hartinger@auckland.ac.nz
**Mario Kubanik, Jason K. Y. Tu, Tilo Söhnel:** School of Chemical Sciences, University of Auckland, Private Bag 92019, Auckland 1142, New Zealand
**Michaela Hejl, Michael A. Jakupec,Wolfgang Kandioller, Bernhard K. Keppler:** University of Vienna, Faculty of Chemistry, Institute of Inorganic Chemistry, Waehringer Str. 42, 1090 Vienna, Austria
**Michael A. Jakupec, Wolfgang Kandioller, Bernhard K. Keppler:** University of Vienna, Research Platform "Translational Cancer Therapy Research", Waehringer Str. 42, A-1090 Vienna, Austria

ligand systems. One of the ligand types used is the class of flavonols which have been coordinated to different metal centers [16-25]. Flavonols are derived from flavones which are naturally occurring constituents of plants, have demonstrated promising tumor-inhibiting activity and are known to be enzyme inhibitors. Flavonoids are a large group of secondary metabolites ubiquitously produced in plants and consist of phenolic fragments possessing two benzene rings linked by heterocyclic systems with one or more hydroxyl groups [26,27]. They are the most abundant polyphenols found in plants and are thought to perform a variety of functions including protection from UV radiation, defense against pathogens, pollinator attraction, pigmentation, and play an essential role in reproduction [28]. Flavonoids have been well-known to exert a wide range of biological properties, including antioxidant, antiradical, antibacterial, estrogenic, antiviral, and also anticancer effects [29-31]. Several *in vitro* studies have shown that phenolics extracted from plants have potential in chemoprevention of hepatoma and melanoma. They may act as cancer blocking agents with their ability to scavenge free radicals, and/or cancer suppressing agents, due to their capacity to target different signal transduction pathways and preventing tumor development by inducing tumor cell apoptosis [32-34].

Flavonols can act as bidentate ligand systems to metal complexes, as has been shown for Ru(II) [20], Zn(II) [25], Cu(II) [21], Pb(II) [22], and Al(III) [23,24] as the metal center. We got interested in the ligand systems as an extension to our early work on hydroxypyrones and -pyridones [35-37], and reported organoruthenium, -osmium and -rhodium [16-19] compounds (Figure 1) with the *p*-fluoro Ru complex **A** (Figure 1, M = Ru, Ar = *p*-cymene, X = Cl, Y = Z = O, R = *p*-F) being among the most potent in *in vitro* assays [16-19]. Complexes of flavonols were found to inhibit topoisomerase IIα while maintaining their coordination ability to DNA model compounds. Topoisomerases are crucial enzymes required for the resolution of topological problems that occur during DNA replication and transcription. This observation supports that the compounds have multitargeted properties. Notably, the complexes were more potent inhibitors of the enzyme than the ligand systems, while the anticancer activity was determined by the flavonoid [16].

Herein, we report the synthesis of 3-hydroxyflavones and their corresponding organometallic Ru(II) complexes, containing electron-withdrawing as well as electron-donating R groups at the phenyl ring (Figure 1), with the aim to get a better understanding of the electronic and structural impact of such substitution on the cytotoxic activity of flavone-derived anticancer agents.

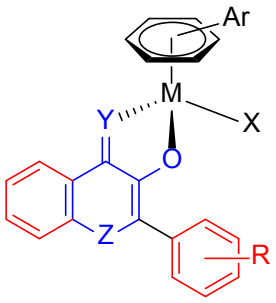


**Figure 1.** General structure of 3-hydroxypyr(id)one-derived organometallic compounds (compound **A**: M = Ru, Ar = *p*-cymene, X = Cl, Y = Z = O, R = *p*-F).

# 2 Experimental

## 2.1 Materials and Methods

All air- and moisture-sensitive reactions were carried out under nitrogen atmosphere using standard Schlenk techniques. Chemicals and solvents were obtained from commercial suppliers and used as received. Tetrahydrofuran (THF) and diethyl ether ($Et_2O$) were first dried through a solvent purification system (LC Technology Solutions Inc., SP-1 solvent purifier) and degassed under a $N_2$ flow, and stored in a Schlenk flask until use. Ethanol (EtOH) and methanol (MeOH) were degassed under $N_2$ and stored for at least a couple of days over activated molecular sieves (3 Å) following a standard procedure [38]. Thin layer chromatography (TLC) was performed with aluminum sheets pre-coated with Merck silica gel 60 $F_{254}$. Detection was achieved by visualization under UV light. Flash column chromatography was employed on silica gel 60, 0.04–0.06 mm (Scharlau). Solvents were evaporated under reduced pressure using a rotary evaporator. 2'-Hydroxyacetophenone (98%) was obtained from AK Scientific, α-terpinene and 3,4,5-trimethoxybenzaldehyde (98%) from Sigma-Aldrich, 3,4-dimethoxybenzaldehyde (99%), 4-acetamidobenzaldehyde (98%), 3,5-dimethoxybenzaldehyde (98%), 2,6-difluorobenzaldehyde (98%), 4-trifluoromethylbenzaldehyde (98%), and sodium (99.8%) from Acros Organics. Sodium methoxide (≥97%) was purchased from Fluka, sodium hydroxide (mini pearls AR), sodium sulfate (anhydrous granular AR), ammonium chloride (AR), molecular sieve 3 Å, acetic acid and sodium acetate (AR) were from ECP, hydrochloric acid (37%) from RCI, ruthenium(III) chloride hydrate (99%) from Precious Metals Online, TLC silica gel 60 $F_{254}$ from Merck, flash chromatography silica gel 60, 0.04–0.06 mm, and sodium chloride (reagent grade) from Scharlau. Bis[($\eta^6$-*p*-cymene)dichloridoru-

thenium(II)] was synthesized as described in the literature [39].

## 2.2 Physical Measurements

NMR spectra were recorded on Bruker DRX 400 MHz NMR spectrometers at ambient temperature, unless otherwise indicated. $^{1}H$ and $^{13}C\{^{1}H\}$ chemical shifts are reported *vs* $SiMe_4$ and were determined by reference to the residual $^{1}H$ and $^{13}C\{^{1}H\}$ solvent peaks. In addition to $^{1}H$ and $^{13}C\{^{1}H\}$ NMR data, some compounds were analyzed via multinuclear 2D ($^{1}H$–$^{1}H$ COSY, $^{1}H$–$^{13}C$ HSQC, and HMBC) NMR spectroscopic experiments, allowing unambiguous assignments of characteristic resonances. Melting points were measured in capillary tubes using a SMP30 Stuart Scientific Melting Point Apparatus. Elemental analyses for all compounds were performed at the Campbell Microanalytical Laboratory, The University of Otago. High resolution mass spectra were recorded on a Bruker microOTOF-Q mass spectrometer in positive ion electrospray ionization (ESI) mode. X-ray diffraction measurements of single crystals were carried out on a Siemens SMART diffractometer with a CCD area detector using graphite monochromated Mo-Kα radiation (λ = 0.71073 A). The data was processed using the SHELX2013 software packages [40]. All non-hydrogen atoms were refined anisotropically. Hydrogen atoms were inserted at calculated positions and refined with a riding model or without restrictions. Molecular structures were visualized using Mercury 3.5.1.

## 2.3 Synthesis

General procedure for 3-hydroxyflavone synthesis **1a–1f**
2'-Hydroxyacetophenone (1.0 eq) was added to a suspension of the respective aldehyde (1.0 eq) in ethanol and aqueous NaOH (5 M, 4.3 eq). The mixture was stirred overnight at room temperature. Afterwards, the reaction mixture was cooled on ice, and aqueous acetic acid (30%) was added until the mixture was acidic. The mixture was stirred for an additional 30 min at 0°C, and the 2'-hydroxychalcone was collected by filtration. Hydrogen peroxide (30%, 2.2 eq) was then added to an ice-cold suspension of the chalcone in ethanol (approx. 100 mL) and NaOH (5 M, 2.0 eq). The mixture was allowed to warm to room temperature and was stirred overnight. The mixture was acidified with 1 M HCl until acidic, and the formed precipitate was collected by filtration. Recrystallization from methanol afforded the flavonols.

*3-Hydroxy-2-(3,4-dimethoxyphenyl)-4H-chromen-4-one (***1a***).* The reaction was performed according to the general procedure by using 3,4-dimethoxybenzaldehyde (2.44 g) to afford **1a** as yellow powder. (1.84 g, 42%); m.p. 182–186°C. $^{1}H$ NMR (400.13 MHz, $d_6$-DMSO): δ = 3.86 (s, 6H, -$OCH_3$), 7.17 (d, $^{3}J(H5',H6')$ = 9 Hz, 1H, H5'), 7.47–7.51 (m, 1H, H6), 7.78–7.80 (m, 2H, H2'/H6'), 7.83 (d, $^{3}J(H7,H8)$ = 2 Hz, 1H, H8), 7.89 (dd, $^{3}J(H6/H8,H7)$ = 8 Hz, $^{4}J(H5,H7)$ = 2 Hz, 1H, H7), 8.11 (dd, $^{3}J(H5,H6)$ = 8 Hz, $^{4}J(H5,H7)$ = 2 Hz, 1H, H5), 9.46 (s, 1H, OH) ppm. $^{13}C\{^{1}H\}$ NMR (100.6 MHz, $d_6$-DMSO): δ = 55.7 (-OMe), 55.6 (-OMe), 111 (C5'), 111.5 (C2'), 118.4 (C8), 121.3 (C4a), 121.5 (C6'), 123.6 (C1'), 124.4 (C5), 124.7 (C6), 133.4 (C7), 138.3 (C3), 145.4 (C2), 148.4 (C3'), 150.3 (C4'), 154.4 (C8a), 172.6 (C4) ppm. MS ($ESI^+$): *m/z* 321.0738 $[M + Na]^+$ ($m_{ex}$ = 321.0722). Elemental Analysis Calculated for $C_{17}H_{14}O_5 \cdot 0.125\ H_2O$: C 67.94, H 4.78%. Found: C 67.98, H 4.78%.

*3-Hydroxy-2-(3,5-dimethoxyphenyl)-4H-chromen-4-one (***1b***).* The reaction was performed according to the general procedure by using 3,5-dimethoxybenzaldehyde (1.67 g) to afford **1b** as yellow powder. (1.60 g, 53%); m.p. 160–163°C. $^{1}H$ NMR (400.13 MHz, $d_6$-DMSO): δ = 3.84 (s, 6H, -$OCH_3$), 6.69 (dd, $^{3}J(H2'/H6',H4')$ = 8 Hz, 1H, H4'), 7.41 (d, $^{4}J(H2'/H6',H4')$ = 2 Hz, 2H, H2'/H6'), 7.48–7.53 (m, 1H, H6), 7.81 (d, $^{3}J(H7,H8)$ = 8 Hz, 1H, H8), 7.82–7.86 (m, 1H, H7), 8.12 (dd, $^{3}J(H5,H6)$ = 8 Hz, $^{4}J(H5,H7)$ = 2 Hz, 1H, H5), 9.46 (s, 1H, OH) ppm. $^{13}C\{^{1}H\}$ NMR (100.6 MHz, $d_6$-DMSO): δ = 55.4 (-OMe), 101.5 (C4'), 106 (C2'/C6'), 118.4 (C8), 121.1 (C4a), 124.5 (C6), 124.7 (C5), 132.9 (C1'), 133.7 (C7), 139.3 (C3), 144.6 (C2), 154.5 (C3'/C5'), 160.4 (8a), 173 (C4) ppm. MS ($ESI^+$): *m/z* 321.0732 $[M + Na]^+$ ($m_{ex}$ = 321.0739). Elemental Analysis Calculated for $C_{17}H_{14}O_5 \cdot 0.2\ H_2O$: C 67.63, H 4.81%. Found: C 67.99, H 5.31%.

*3-Hydroxy-2-(3,4,5-trimethoxyphenyl)-4H-chromen-4-one (***1c***).* The reaction was performed according to the general procedure by using 3,4,5-trimethoxybenzaldehyde (2.88 g) to afford **1c** as yellow powder. (3.14 g, 65%); m.p. 179–181°C. $^{1}H$ NMR (400.13 MHz, $d_6$-DMSO): δ = 3.77 (s, 3H, $CH_3$), 3.88 (s, 6H, $CH_3$), 7.48–7.53 (m, 1H, H6), 7.57–7.63 (m, 2H, H7/H8), 7.79–7.84 (m, 2H, H2'/H6'), 8.12 (dd, $^{3}J(H5,H6)$ = 8 Hz, $^{4}J(H5,H7)$ = 2 Hz, 1H, H5), 9.59 (s, 1H, OH) ppm. $^{13}C\{^{1}H\}$ NMR (100.6 MHz, $d_6$-DMSO): δ = 56.0 ($CH_3$), 60.2 ($CH_3$), 105.6 (C2'/C6'), 118.5 (C5), 121.2 (C8), 124.5 (C4a), 124.7 (C6), 126.5 (C7), 133.5 (C1'), 138.8 (C2), 139.2 (C4'), 144.9 (C8a), 152.7 (C3), 154.4 (C3'/C5'), 172.8 (C4) ppm. MS ($ESI^+$): *m/z* 351.0844 $[M + Na]^+$ ($m_{ex}$ = 351.0846). Elemental Analysis Calculated for $C_{18}H_{16}O_6 \cdot 0.125\ H_2O$: C 65.40, H 4.95%. Found: C 65.38, H 5.15%.

*3-Hydroxy-2-(2,6-difluorophenyl)-4H-chromen-4-one (***1d***)*. The reaction was performed according to the general procedure by using 2,6-difluorobenzaldehyde (2.09 g) to afford **1d** as milky powder (2.09 g, 55%); m.p. 210–213°C. $^1$H NMR (400.13 MHz, $d_6$-DMSO): δ = 7.33 (dd, $^3J$*(H3'/H5',H4')* = 8 Hz, 2H, H3'/H5'), 7.52 (dd, $^3J$*(H5/H7,H6)* = 8 Hz, 1H, H6), 7.70–7.76 (m, 2H, H4', H8), 7.83–7.86 (m, 1H, H7), 8.18 (dd, $^3J$*(H5,H6)* = 8 Hz, $^4J$*(H5,H7)* = 2 Hz, 1H, H5), 9.69 (s, 1H, OH) ppm. $^{13}$C{$^1$H} NMR (100.6 MHz, $d_6$-DMSO): δ = 111.9 (C3'/C5'), 112.2 (C8), 118.4 (C4a), 121.5 (C6), 124.9 (C5), 125.1 (C1'), 134.1 (C4'), 138.2 (C7), 140.9 (C3), 155.2 (C2'/C6'), 158.4 (C8a), 160.9 (C2), 172.6 (C4) ppm. MS (ESI$^+$): *m/z* 297.0329 [M + Na]$^+$ ($m_{ex}$ = 297.0339). Elemental Analysis Calculated for $C_{15}H_8F_2O_3 \cdot 0.5\ H_2O$: C 63.61, H 3.20%. Found: C 63.69, H 2.95%.

*3-Hydroxy-2-(4-(trifluoromethyl)phenyl)-4H-chromen-4-one (***1e***)*. The reaction was performed according to the general procedure by using 4-trifluoromethylbenzaldehyde (2.58 g) to afford **1e** as yellow powder (3.60 g, 80%); m.p. 181–184°C. $^1$H NMR (400.13 MHz, $d_6$-DMSO): δ = 7.48–7.52 (m, 1H, H6), 7.82–7.86 (m, 2H, H3/H5), 7.95 (d, $^3J$*(H2'/H6',H3'/H5')* = 8 Hz, 2H, H3'/H5'), 8.15 (dd, $^3J$*(H5,H6)* = 8 Hz, $^4J$*(H5,H7)* = 2 Hz, 1H, H5), 8.45 (d, $^3J$*(H2'/H6',H3'/H5')*= 8 Hz, 2H, H2'/H6'), 10.04 (s, 1H, OH) ppm. $^{13}$C{$^1$H} NMR (100.6 MHz, $d_6$-DMSO): δ = 118.5 (C8), 121.3 (C4a), 124.7 ($CF_3$), 124.8 (C6), 125.4 (C5), 128.2 (C3'/C5'), 129.2 (C4'), 129.5 (C1'), 134.1 (C2'/C6'), 135.3 (C7), 140.1 (C3), 143.3 (C2), 154.6 (C8a), 173.2 (C4) ppm. MS (ESI$^+$): *m/z* 329.0397 [M + Na]$^+$ ($m_{ex}$ = 329.0401). Elemental Analysis Calculated for $C_{16}H_9F_3O_3$: C 62.75, H 2.96%. Found: C 62.91, H 2.95%.

*3-Hydroxy-2-(4-acetomidophenyl)-4H-chromen-4-one (***1f***)*. The reaction was performed according to the general procedure by using 4-acetomidobenzaldehyde (1.63 g) to afford **1f** as dark yellow crystals. (2.18 g, 74%); m.p. 260–262°C. $^1$H NMR (400.13 MHz, $d_6$-DMSO): δ = 2.09 (s, 3H, $CH_3$), 7.47–7.53 (m, 1H, H7), 7.74–7.82 (m, 4H, H6, H8, H3'/H5'), 8.12 (dd, $^3J$*(H5,H6)* = 8 Hz, $^4J$*(H5,H7)* = 2 Hz, 1H, H5), 8.20 (d, $^3J$*(H2'/H6',H3'/H5')* = 8 Hz, 2H, H2'/H6'), 9.51 (s, 1H, OH), 10.22 (s, 1H, NH) ppm. $^{13}$C{$^1$H} NMR (100.6 MHz, $d_6$-DMSO): δ = 24.1 ($CH_3$), 118.3 (C8), 118.5 (C3'/C5'), 121.3 (C8a), 124.5 (C6), 124.7 (C5), 125.6 (C1'), 128.4 (C2'/C6'), 133.4 (C7), 138.5 (C3), 140.7 (C4'), 145.3 (C2), 154.5 (C4a), 168.7 (C=O), 172.7 (C4) ppm. MS (ESI$^+$): *m/z* 318.0747 [M + Na]$^+$ ($m_{ex}$ = 318.0742). Elemental Analysis Calculated for $C_{17}H_{13}NO_4 \cdot 0.4\ H_2O$: C 67.50, H 4.60, N 4.63%. Found: C 67.63, H 4.52, N 4.70%.

General procedure for the synthesis of [($\eta^6$-*p*-cymene)Ru$^{II}$] complexes **2a**–**2f**

[($\eta^6$-*p*-cymene)$RuCl_2$]$_2$ (50 mg, 0.90 eq) was added to a solution of the respective 3-hydroxyflavone **1a–1f** (1.0 eq) and sodium methoxide (11 mg, 1.1 eq) in dry methanol (10 mL). The reaction mixture was stirred at room temperature under nitrogen atmosphere for 2–8hours. Afterwards the reaction mixture was concentrated under reduced pressure, the residue dissolved in dichloromethane, and filtered and precipitated with n-hexane. Pure compound was obtained by recrystallization from methanol. Single crystals for X-ray diffraction analysis were obtained by crystallization from chloroform/n-hexane.

*Chlorido[3-(oxo-κO)-2-(3,4-dimethoxyphenyl)-chromen-4-onato-κO](η$^6$-p-cymene)ruthenium(II) (***2a***)*. The synthesis was performed according to the general procedure using **1a** (54 mg) to afford a red solid (86 mg, 84%). m.p. 197°C (decomp.). $^1$H NMR (400.13 MHz, $CDCl_3$): δ = 1.41 (dd, $^3J$*(He,Hf)* = 7 Hz, $^3J$*(He,Hf)* = 7 Hz, 6H, H*f*), 2.40 (s, 3H, H*g*), 2.89–2.99 (m, 1H, H*e*), 3.96 (s, 3H, -OMe), 4.00 (s, 6H, -OMe), 5.33–5.38 (m, 2H, H*b*), 5.62–5.66 (m, 2H, H*c*), 6.97 (d, $^3J$*(H5',H6')* = 8 Hz, 1H, H5'), 7.30–7.34 (m, 1H, H6), 7.53 (d, $^3J$*(H7,H8)* = 8 Hz, 1H, H8), 7.55–7.60 (m, 1H, H7), 8.19 (dd, $^3J$*(H5,H6)* = 8 Hz, $^4J$*(H5,H7)* = 2 Hz, 1H, H5), 8.19–8.23 (m, 2H, H2'/H6') ppm. $^{13}$C{$^1$H} NMR (100.6 MHz, $CDCl_3$): δ = 18.7 (C*g*), 22.5 (C*f*), 31.3 (C*e*), 55.9 (-OMe), 78.1 (C*b*), 80.7 (C*c*), 95.5 (C*a*), 98.8 (C*d*), 110.5 (C5'), 110.8 (C2'), 117.7 (C8), 120.1 (C4a), 121.3 (C6'), 123.9 (C1'), 124.5 (C5), 125.5 (C6), 132.2 (C7), 148.5 (C3), 149.7 (C2), 150.3 (C3'), 153.6 (C4'), 153.8 (C8a), 182.5 (C4) ppm. MS (ESI$^+$): *m/z* 533.0925 [M – Cl]$^+$ ($m_{ex}$ = 533.0902). Elemental Analysis Calculated for $C_{27}H_{27}ClO_5Ru \cdot 1.3\ CHCl_3$: C 47.00, H 3.94%. Found: C 46.73, H 3.97%.

*Chlorido[3-(oxo-κO)-2-(3,5-dimethoxyphenyl)-chromen-4-onato-κO](η$^6$-p-cymene)ruthenium(II) (***2b***)*. The synthesis was performed according to the general procedure using **1b** (54 mg) to afford a red solid (75 mg, 73%). m.p. 201°C (decomp.). $^1$H NMR (400.13 MHz, $CDCl_3$): δ = 1.42 (dd, $^3J$*(He,Hf)* = 7 Hz, $^3J$*(He,Hf)* = 7 Hz, 6H, H*f*), 2.40 (s, 3H, H*g*), 2.90–3.00 (m, 1H, H*e*), 3.88 (s, 6H, -OMe), 5.33–5.38 (m, 2H, H*b*), 5.62–5.68 (d, 2H, H*c*), 6.53 (dd, $^3J$*(H2'/H6',H4')* = 8 Hz, 1H, H4'), 7.28–7.35 (m, 1H, H6), 7.53 (d, $^3J$*(H7,H8)* = 8 Hz, 1H, H8), 7.56–7.63 (m, 1H, H7), 7.80 (d, $^4J$*(H2'/H6',H4')* = 2 Hz, 2H, H2'/H6'), 8.20 (dd, $^3J$*(H5,H6)* = 8 Hz, $^4J$*(H5,H7)* = 2 Hz, 1H, H5) ppm. $^{13}$C{$^1$H} NMR (100.6 MHz, $CDCl_3$): δ = 18.6 (C*g*), 22.5 (C*f*), 31.3 (C*e*), 55.5 (d, -OMe), 78.2 (C*b*), 80.8 (C*c*), 95.5 (C*a*), 98.8 (C*d*), 102.0 (C4'), 105.5 (C2'/C6'), 117.9 (C8), 119.9 (C4a), 124.0 (C6), 124.6 (C5), 132.7 (C1'), 134.2 (C7),

153.4 (C2), 154.8 (C3'/C5'), 160.5 (C8a), 183.5 (C4) ppm. MS (ESI$^+$): *m/z* 533.0902 [M − Cl]$^+$ ($m_{ex}$ = 533.0902). Elemental Analysis Calculated for $C_{27}H_{27}ClO_5Ru{\cdot}0.25\ H_2O$: C 56.64, H 4.84%. Found: C 56.38, H 4.69%.

*Chlorido[3-(oxo-κO)-2-(3,4,5-trimethoxyphenyl)-chromen-4-onato-κO](η$^6$-p-cymene) ruthenium(II)* (**2c**). The synthesis was performed according to the general procedure using **1c** (60 mg) to afford a deep red solid (70 mg, 70%); m.p. 220°C (decomp.). $^1$H NMR (400.13 MHz, $CDCl_3$): δ = 1.42 (dd, $^3$*J(He,Hf)* = 7 Hz, $^3$*J(He,Hf)* = 7 Hz, 6H, H*f*), 2.40 (s, 3H, H*g*), 2.90–3.01 (m, 1H, H*e*), 3.92 (s, 3H, -OMe), 3.98 (s, 6H, -OMe), 5.33–5.38 (m, 2H, H*b*), 5.60–5.66 (m, 2H, H*c*), 7.30–7.35 (m, 1H, H7), 7.54 (d, $^3$*J(H7,H8)* = 8 Hz, 1H, H8), 7.56–7.61 (m, 1H, H6), 7.89 (s, 2H, H2'/H6'), 8.19 (dd, $^3$*J(H5,H6)* = 8 Hz, $^4$*J(H5,H7)* = 2 Hz, 1H, H5) ppm. $^{13}$C{$^1$H} NMR (100.6 MHz, $CDCl_3$): δ = 18.6 (C*g*), 22.5 (C*f*), 31.4 (C*e*), 56.2 (-OMe), 61.0 (-OMe), 78.3 (C*b*), 80.7 (C*c*), 95.2 (C*a*), 98.7 (C*d*), 105.1 (C2'/C6'), 117.7 (C5), 120.0 (C8), 124.1 (C4a), 124.6 (C6), 127.9 (C7), 132.5 (C1'), 139.6 (C2), 149.1 (C8a), 152.9 (C3), 153.7 (C3'), 154.3 (C5'), 183.1 (C4) ppm. MS (ESI$^+$): *m/z* 563.1032 [M − Cl]$^+$ ($m_{ex}$ = 563.1007). Elemental Analysis Calculated for $C_{28}H_{29}ClO_6Ru{\cdot}CHCl_3$: C 48.55, H 4.21%. Found: C 48.37, H 4.39%.

*Chlorido[3-(oxo-κO)-2-(2,6-difluorophenyl)-chromen-4-onato-κO](η$^6$-p-cymene)ruthenium(II)* (**2d**). The synthesis was performed according to the general procedure using **1d** (50 mg) to afford a red solid (74 mg, 75%). m.p. 237°C (decomp.). $^1$H NMR (400.13 MHz, $CDCl_3$): δ = 1.35 (dd, $^3$*J(He,Hf)* = 7 Hz, $^3$*J(He,Hf)* = 7 Hz, 6H, H*f*), 2.35 (s, 3H, H*g*), 2.85–2.96 (m, 1H, H*e*), 5.33–5.38 (m, 2H, H*b*), 5.59–5.63 (m, 2H, H*c*), 6.92–6.98 (m, 2H, H3'/H5'), 7.31–7.34 (m, 1H, H6), 7.37–7.43 (m, 1H, H4'), 7.45–7.50 (m, 1H, H8), 7.57–7.63 (m, 1H, H7), 8.24 (dd, $^3$*J(H5,H6)* = 8 Hz, $^4$*J(H5,H7)* = 2 Hz, 1H, H5) ppm. $^{13}$C{$^1$H} NMR (100.6 MHz, $CDCl_3$): δ = 18.6 (C*g*), 22.4 (C*f*), 31.0 (C*e*), 77.5 (C*b*), 80.5 (C*c*), 96.7 (C*a*), 99.7 (C*d*), 111.6 (C3'/C5'), 111.8 (C8), 120.2 (C4a), 124.1 (C6), 124.8 (C5), 131.4 (C4'), 133.9 (C7), 141.5 (C3), 155.0 (C8a), 155.1 (C1'), 159.8 (C6'), 162.4 (C2'), 183.8 (C4) ppm. MS (ESI$^+$): *m/z* 509.0515 [M − Cl]$^+$ ($m_{ex}$ = 509.0502). Elemental Analysis Calculated for $C_{25}H_{21}ClF_2O_3Ru{\cdot}0.9CHCl_3$: C 47.76, H 3.39%. Found: C 47.96, H 3.44%.

*Chlorido[3-(oxo-κO)-2-(4-trifluoromethylphenyl)-chromen-4-onato-κO](η$^6$-p-cymene)ruthenium(II)* (**2e**). The synthesis was performed according to the general procedure using **1e** (56 mg) to afford a red solid (81 mg, 75%). m.p. 240°C (decomp.). $^1$H NMR (400.13 MHz, $CDCl_3$): δ = 1.37–1.46 (m, 6H, H*f*), 2.41 (s, 3H, H*g*), 2.95–3.05 (m, 1H, H*e*), 5.35–5.43 (m, 2H, H*b*), 5.62–5.71 (m, 2H, H*c*), 7.31–7.36 (m, 1H, H6), 7.53–7.57 (m, 1H, H8), 7.60–7.66 (m, 1H, H7), 7.70 (d, $^3$*J(H2'/H6',H3'/H5')* = 8 Hz, 2H, H3'/H5'), 8.21 (dd, $^3$*J(H5,H6)* = 8 Hz, $^4$*J(H5,H7)* = 2 Hz, 1H, H5), 8.69 (d, $^3$*J(H2'/H6',H3'/H5')* = 8 Hz, 2H, H2'/H6') ppm. $^{13}$C{$^1$H} NMR (100.6 MHz, $CDCl_3$): δ = 18.7 (C*g*), 22.4 (C*f*), 31.3 (C*e*), 78.0 (C*b*), 81.0 (C*c*), 96.0 (C*a*), 99.1 (C*d*), 117.9 (C8), 120.0 (C4a), 124.3 ($CF_3$), 124.8 (C6), 125.1 (C5), 127.1 (C3'/C5'), 129.7 (C4'), 130.0 (C1'), 130.3 (C2'), 133.2 (C6'), 135.9 (C7), 147.0 (C3), 154.2 (C2), 155.3 (C8a), 184.2 (C4) ppm. MS (ESI$^+$): *m/z* 541.0588 [M − Cl]$^+$ ($m_{ex}$ = 541.0564). Elemental Analysis Calculated for $C_{26}H_{22}ClF_3O_3Ru{\cdot}0.75\ H_2O$: C 52.98, H 4.02%. Found: C 52.84, H 3.71%.

*Chlorido[3-(oxo-κO)-2-(4-acetomidophenyl)-chromen-4-onato-κO](η$^6$-p-cymene)ruthenium(II)* (**2f**). The synthesis was performed according to the general procedure using **1f** (54 mg) to afford a red solid (56 mg, 55%). m.p. 270°C (decomp.). $^1$H NMR (400.13 MHz, $CDCl_3$): δ = 1.41 (dd, $^3$*J(He,Hf)* = 7 Hz, $^3$*J(He,Hf)* = 7 Hz, 6H, H*f*), 1.97 (s, 3H, $CH_3$), 2.41 (s, 3H, H*g*), 2.88–2.98 (m, 1H, H*e*), 5.34–5.38 (m, 2H, H*b*), 5.62–5.66 (m, 2H, H*c*), 7.30–7.37 (m, 2H, H3'/H5'), 7.50–7.63 (m, 3H, H6,H7,H8), 7.72 (brs, 1H, NH), 8.18 (dd, *3J(H5,H6)* = 8 Hz, $^4$*J(H5,H7)* = 2 Hz, 1H, H5), 8.44 (d, *3J(H2'/H6',H3'/H5')* = 8 Hz, 2H, H2'/H6') ppm. MS (ESI$^+$): *m/z* 530.0916 [M − Cl]$^+$ ($m_{ex}$ = 530.0905). Elemental Analysis Calculated for $C_{27}H_{26}ClNO_4Ru{\cdot}1.75\ H_2O$: C 54.36, H 4.98, N 2.35 %. Found: C 54.23, H 4.61%, N 2.40%.

## 2.4 In vitro anticancer activity

*Cell lines and culture conditions.* CH1 cells (identified via STR profiling as PA-1 ovarian teratocarcinoma cells by Multiplexion, Heidelberg, Germany; see also [41]) were obtained from Lloyd R. Kelland, CRC Centre for Cancer Therapeutics, Institute of Cancer Research, Sutton, UK. SW480 (human adenocarcinoma of the colon) and A549 (human non-small cell lung cancer) cells were provided by Brigitte Marian (Institute of Cancer Research, Department of Medicine I, Medical University of Vienna, Austria). Cells were grown in 75 cm² culture flasks as adherent monolayer cultures in Minimal Essential Medium (MEM) supplemented with 10% heat-inactivated fetal calf serum, 1 mM sodium pyruvate, 4 mM l-glutamine and 1% non-essential amino acids (100×). Cultures were maintained at 37°C in a humidified atmosphere containing 95% air and 5% $CO_2$.

*MTT assay conditions.* Cytotoxicity was determined by the colorimetric MTT (3-(4,5-dimethyl-2-thiazolyl)-2,5-diphenyl-2H-tetrazolium bromide) microculture assay. For this purpose, cells were harvested from culture flasks by

trypsinization and seeded in 100 µL aliquots into 96–well microculture plates. Cell densities of $1.5 \times 10^3$ cells/well (CH1), $2.5 \times 10^3$ cells/well (SW480) and $4 \times 10^3$ cells/well (A549) were chosen in order to ensure exponential growth of untreated controls throughout the experiment. Cells were allowed to settle and resume exponential growth in drug-free complete culture medium for 24 h. Stocks of the test compounds in DMSO were appropriately diluted in complete culture medium such that the maximum DMSO content did not exceed 1%. The dilution was added in 100 µL aliquots to the microcultures and cells were exposed to the test compounds for 96 hours. At the end of exposure, all media were replaced by 100 µL/well RPMI1640 culture medium (supplemented with 10% heat-inactivated fetal bovine serum) plus 20 µL/well MTT solution in phosphate-buffered saline (5 mg/mL). After incubation for 4 h, the supernatants were removed, and the formazan crystals formed by viable cells were dissolved in 150 µL DMSO per well. Optical densities at 550 nm were measured with a microplate reader, using a reference wavelength of 690 nm to correct for unspecific absorption. The quantity of viable cells was expressed relative to untreated control microcultures, and 50% inhibitory concentrations ($IC_{50}$) were calculated from concentration-effect curves by interpolation. Evaluation is based on means from at least three independent experiments, each comprising at least three replicates per concentration level.

## 2.5 Lipophilicity

ChemBioDrawUltra 12.0 and software tools from Molinspiration (http://www.molinspiration.com) and VCCLAB (Virtual Computational Chemistry Laboratory, http://www.vcclab.org, 2005) were used to estimate the compounds' lipophilicity based on calculated logarithmic octanol–water partition coefficients (clog*P*) for the ligands **1a**–**1f** [42]. The ligands were chosen for the calculations since the Ru($\eta^6$-*p*-cymene)Cl moiety is present in all complexes.

## 2.6 Solubility

DMSO stock solutions of the compounds were used to determine the solubility in α-MEM medium, supplemented with 5% fetal calf serum (FCS), by adding 1 vol% of the stock solution to an appropriate amount of medium. In a standard experiment, 2.5 µL of the DMSO stock was added to 247.5 µL of medium. If precipitation was observed, the experiment was repeated with a decreased concentration of the compound in DMSO, for example by diluting 2.5 µL of the DMSO stock with another 2.5 µL of DMSO, and this solution was then added to 495 µL of medium. This process was repeated until no precipitation was observed.

# 3 Results and Discussion

3-Hydroxyflavones (3-HFs) have shown remarkable activity in medicinal applications, and the modification of 3-hydroxyflavones has widened the bioavailability. In order to make them suitable to coordinate to metal centers, a series of substituted 3-hydroxyflavones was synthesized. A Claisen-Schmidt condensation of various substituted benzaldehydes and 2'-hydroxyacetophenone in the presence of aqueous sodium hydroxide gave the corresponding chalcones (Scheme 1). A subsequent Algar-Flynn-Oyamada reaction with alkaline hydrogen peroxide produced the substituted 3-HFs **1a–f** in yields of 25–80% [43].

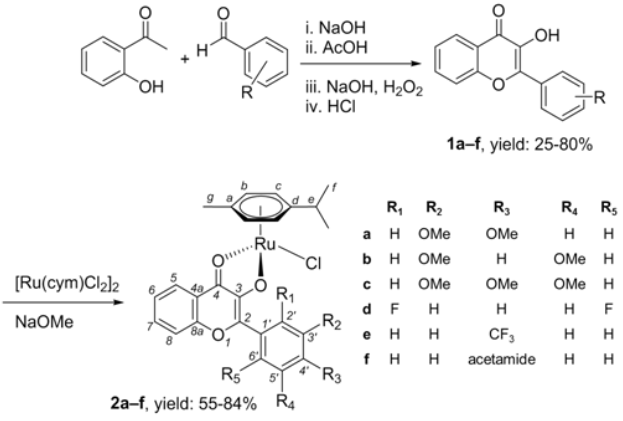


**Scheme 1.** Synthesis of 3-hydroxyflavonol ligands and the respective Ru(cym)Cl complexes.

To obtain the ruthenium complexes **2a–2f**, 3-hydroxyflavones **1a–1f** (1.0 eq) and sodium methoxide (1.1 eq) were dissolved in dry methanol and stirred for 10 min (Scheme 1). This results in deprotonation of the 3-HF and allows reaction with dimeric [($\eta^6$-*p*-cymene)$RuCl_2$]$_2$ (0.90 eq) dimer, under cleavage of the chloride bridge to yield neutral [Ru(cym)Cl] (cym = $\eta^6$-*p*-cymene) complexes (yield: 55–85%).

All ligands were characterized by melting point, $^1$H NMR and $^{13}$C{$^1$H} NMR spectroscopy in $d_6$-DMSO. New ligands were further analyzed by ESI-MS, and elemental analysis.

The $^1$H NMR spectra featured the hydroxyl protons generally around 9.10–9.40 ppm [16]. The signals of the phenolic protons from 3-HFs are slightly shifted, due to

the different strength electronic effects of the substituents on the phenyl rings. The protons of the methyl group of ligand **1f** appear at 2.09 ppm (singlet), whereas the protons from the methoxy group of ligands **1a–c** give a singlet in the range of 3.80–3.90 ppm. This is due to the presence of the electronegative oxygen atom which results in a downfield shift of the methyl protons. $^{13}C\{^1H\}$ NMR spectroscopy shows the C=O carbon signal generally around 173 ppm for all ligands. The methyl group of **1f** appears at 24.1 ppm, which is in the typical range of alkyl groups. Signals for the methoxy carbon atoms of **1a–c** are typically located around 56 ppm. Fluoro-substituted ligands (**1d**, **1e**) showed additional coupling to the C1', C2'/C6, C3'/C5' and C4' carbon atoms.

The complexes were characterized by melting point, $^1H$ and $^{13}C\{^1H\}$ NMR spectroscopy, mass spectrometry, elemental analysis and single crystal X-ray diffraction analysis. Complexes **2a**, **2d** and **2e** contained $CHCl_3$ as determined by elemental analysis which may contribute to their cytotoxicity. However, **2b** was the most cytotoxic compound in the series (see below). Some characteristic features for 3-HF ligands and their complexes were unequivocally identified by 1D NMR spectroscopy in $CDCl_3$. The chemical shifts of the complexes are very close to that of the corresponding ligand. However, due to the electron-withdrawing effect induced by the ruthenium center, the signals appear slightly down-field in the spectra of the complexes as compared to free ligands. The protons of the two methyl groups of cymene (H*f*) give rise to two doublets in the $^1H$ NMR spectra at *ca*. 1.4 ppm, each integrating for 3 protons, whereas the protons of the methyl group H*g* are found at *ca*. 2.4 ppm (singlet). The proton H*e* resonates at *ca*. 3.0 ppm. The proton signals of H*b* and H*c* of the arene region are observed in two regions (*ca*. 5.4 and 5.6 ppm) as multiplets, with a total integral of four protons. In the $^{13}C\{^1H\}$ NMR spectra, the two methyl carbons C*f* resonate at *ca*. 23 ppm, and C*g* is found at 19 ppm. Both of these signals are in the typical range of primary alkyl groups. C*e* is detected at *ca*. 31 ppm, while both aromatic cymene carbons C*b* and C*c* appear at *ca*. 78 and 81 ppm, respectively. The signals for the two quaternary carbon atoms C*a* and C*d* were assigned in the $^{13}C\{^1H\}$ NMR spectra with the aid of HMBC spectra.

Single crystals of **2b**–**2e** suitable for X-ray diffraction analysis were obtained by crystallization from chloroform/n-hexane (Figure 2). The enantiomeric mixtures of all the Ru(II) compounds crystallized in the pseudo-tetrahedral "piano-stool" configuration with a π-bound *p*-cymene

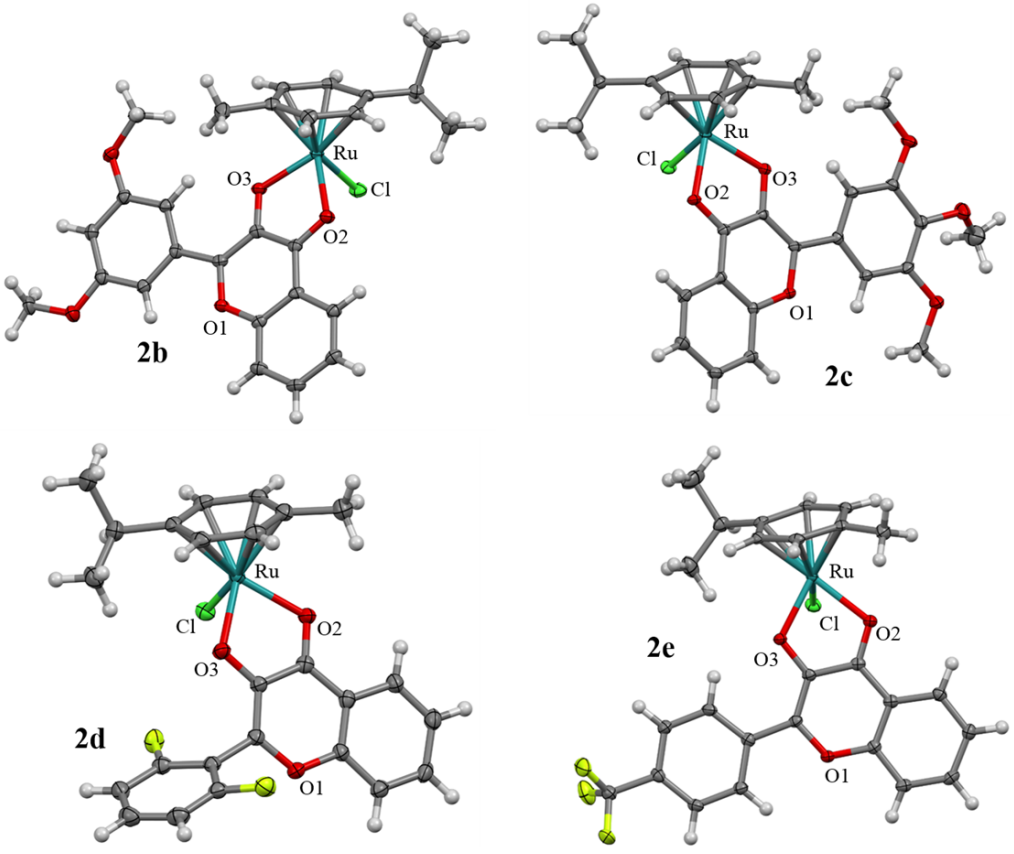


**Figure 2.** ORTEP diagram of one of two enantiomers found in the molecular structures of **2b–2e**. The thermal ellipsoids were set at 50% probability and solvent molecules in the structures of **2c** and **2d** were deleted for clarity.

ring forming the seat through coordination in $\eta^6$ fashion to the Ru center and the ligands act as the legs. Complex **2b** crystallized in the triclinic centrosymmetric space group *P*-1, whereas the other three compounds crystallized in monoclinic cells with the space groups $P2_1/c$ (**2c**), $C2/c$ (**2d**) and $P2_1/n$ (**2e**) (Table 1).

The 3-hydroxyflavone ligand binds bidentately to the ruthenium center, forming a non-planar, envelope-like five-membered cycle. The *meta* and *para* substituted phenyl rings of the flavone ligands show in the X-ray structures small torsion angles, whereas the *ortho* substitution of complex **2d** results in a twisted phenyl ring with a torsion angle of 60.22°

**Table 1.** Details of collected X-ray data for complexes **2b–2e**

| | **2b** | **2c** | **2d** | **2e** |
|---|---|---|---|---|
| Formula | $C_{27}H_{27}ClO_5Ru$ | $C_{28}H_{29}ClO_6Ru \bullet 3CHCl_3$ | $C_{25}H_{21}ClF_2O_3Ru \bullet 0.5CHCl_3$ | $C_{26}H_{22}ClF_3O_3Ru$ |
| CCDC Nr. | 1402549 | 1402550 | 1402551 | 1402552 |
| Molecular weight (g mol$^{-1}$) | 568.01 | 598.05 | 543.95 | 575.96 |
| Temperature (K) | 100(2) | 99(2) | 101(2) | 100(2) |
| Wavelength (Å) | 0.71073 | 0.71073 | 0.71073 | 0.71073 |
| Crystal system | Triclinic | Monoclinic | Monoclinic | Monoclinic |
| Space group | *P*-1 | $P2_1/c$ | $C2/c$ | $P2_1/n$ |
| a (Å) | 8.9186(5) | 15.4715(10) | 22.9901(9) | 9.7631(4) |
| b (Å) | 12.0214(7) | 17.6062(11) | 11.9033(5) | 10.3130(5) |
| c (Å) | 13.1440(8) | 15.0190(9) | 19.5172(8) | 22.9814(10) |
| α (°) | 99.220(4) | 90 | 90 | 90 |
| β (°) | 108.583(3) | 111.494(3) | 113.802(2) | 101.528(2) |
| γ (°) | 110.975(3) | 90 | 90 | 90 |
| Volume (Å$^3$) | 1185.82(12) | 3806.6(4) | 4886.8(4) | 2267.25(18) |
| Z | 2 | 4 | 8 | 4 |
| Calculated density (g cm$^{-3}$) | 1.591 | 1.668 | 1.479 | 1.687 |
| Absorption coefficient (mm$^{-1}$) | 0.811 | 1.155 | 0.789 | 0.861 |
| F(000) | 580 | 1920 | 2192 | 1160 |
| Crystal size (mm × mm × mm) | 0.38 × 0.28 × 0.20 | 0.4 × 0.4 × 0.3 | 0.38 × 0.10 × 0.05 | 0.22 × 0.20 × 0.18 |
| 2θ (min, max) (°) | 1.72, 27.94 | 1.83, 28.11 | 1.94, 27.88 | 1.81, 27.88 |
| Limiting indices | -11 ≤ h ≤ 11,<br>-15 ≤ k ≤ 15,<br>-17 ≤ l ≤ 17 | -20 ≤ h ≤ 20,<br>-23 ≤ k ≤ 23,<br>-19 ≤ l ≤ 19 | -30 ≤ h ≤ 30,<br>-15 ≤ k ≤ 15,<br>-19 ≤ l ≤ 25 | -12 ≤ h ≤ 12,<br>-13 ≤ k ≤ 13,<br>-30 ≤ l ≤ 30 |
| Reflections collected / unique | 27231 / 5614 [R(int) = 0.0559] | 83035 / 9183 [R(int) = 0.0800] | 29504 / 5804 [R(int) = 0.0627] | 28277 / 5376 [R(int) = 0.0404] |
| Completeness to theta = 25.24 | 98.8% | 99.9% | 99.8% | 100.0% |
| Data / restraints / parameters | 5614 / 0 / 328 | 9183 / 0 / 471 | 5804 / 0 / 324 | 5376 / 0 / 330 |
| Goodness-of-fit on F$^2$ [a)] | 1.083 | 1.061 | 1.068 | 1.030 |
| Final R indices [I>2σ(I)] [b)] | $R_1$ = 0.0356,<br>$wR_2$ = 0.1047 | $R_1$ = 0.0548,<br>$wR_2$ = 0.1509 | $R_1$ = 0.0374,<br>$wR_2$ = 0.0823 | $R_1$ = 0.0251,<br>$wR_2$ = 0.0609 |
| R indices (all data) | $R_1$ = 0.0470,<br>$wR_2$ = 0.1097 | $R_1$ = 0.0711,<br>$wR_2$ = 0.1677 | $R_1$ = 0.0553,<br>$wR_2$ = 0.0908 | $R_1$ = 0.0298,<br>$wR_2$ = 0.0637 |
| Largest diff. peak and hole (eÅ$^{-3}$) | 1.539 and -0.621 | 3.677 and -1.766 | 0.890 and -0.997 | 0.579 and -0.343 |

a) GOF = $\{\sum[w(F_o^2 - F_c^2)^2]/(n-p)\}^{1/2}$, where $n$ is the number of reflections and $p$ is the total number of parameters refined.

b) $R_1 = \sum||F_o| - |F_c||/\sum|F_o|$ . $wR_2 = \{\sum[w(F_o^2 - F_c^2)^2]/\sum[w(F_o^2)^2]\}^{1/2}$ .

(Table 2). Due to the small torsion angles of the *meta* and *para* substituted flavones, π-stacking of the aromatic ligands was observed with the other enantiomer present in the crystal structure (Figure 3) All four compounds show Ru–O bond lengths in the ranges of 2.101(3)–2.1197(19) and 2.067(2)–2.093(2) Å for the Ru–O2 and Ru–O3 bonds, respectively, which is in good agreement with the literature. Table 2 summarizes selected features of the Ru complexes **2b–2e** in comparison to reported Ru(arene)(flavonol) complexes [16]. The majority of the bond lengths and angles involving the ruthenium center and oxygen atoms and chlorido ligands are very similar as well as the distance between the ruthenium center to centroid$_{cymene}$. The most significant differences were observed for the torsion angles at C(3)–C(2)–C(1')–C(2'), where different substituents induce rotation of the phenyl ring around the C(2)–C(1') bond. This results in almost co-planar configuration for phenyl rings with substituents in *meta* and *para* positions, while substituents in *ortho* position induce a twist towards an orthogonal position to the flavonoid backbone of the ligand.

Lipophilicity is regarded as a supportive factor for high anticancer activity at least in an *in vitro* setting, as it influences the ability of a drug to penetrate through the cell membrane and accumulate in cells. In order to compare the lipophilic properties of the organoruthenium compounds developed, we compared the clog*P* values of the flavonol ligands, as the Ru(cym)Cl component is present in all studied compounds and the coordination geometries around the Ru center, as apparent from the X-ray diffraction studies, are very similar. We used three widely used software solutions, *i.e.*, ChemDraw, Molinspiration and ALOGPS 2.1, for the calculation of clog*P* values of **1a**–**1f** and compared the values to that of the *p*-fluoro-substituted 3-hydroxyflavone (**A**$_{flavone}$) as the ligand in the most cytotoxic Ru(cym)(HF)Cl complex **A** (Figure 1). While the values obtained from the different software solutions are varying, the trends are very similar in each set of calculations with **1e** being the most lipophilic compound (and the least soluble in 1% DMSO/medium mixture; Table 4) and **1f** being the least lipophilic in the series while **A**$_{flavone}$ shows intermediate clog*P* values.

**Table 2.** Selected bond lengths (Å) and angles (°) for complexes **2b–2e** as compared to the reported ruthenium-*p*-cymene complex with 2-chloro substituted flavone ligand [16].

| Compound | 2b | 2c | 2d | 2e | 2-chloro |
|---|---|---|---|---|---|
| **Bond Lengths** (Å) | | | | | |
| Ru–O(2) | 2.103(2) | 2.101(3) | 2.1197(19) | 2.1193(13) | 2.134(2) |
| Ru–O(3) | 2.067(2) | 2.077(3) | 2.093(2) | 2.0730(12) | 2.087(2) |
| Ru–Cl | 2.4161(10) | 2.4202(9) | 2.4159(8) | 2.4196(5) | 2.410(7) |
| Ru–centroid$_{arene}$ | 1.634 | 1.646 | 1.643 | 1.643 | 1.647 |
| **Torsion Angles (°)** | | | | | |
| C(3)–C(2)–C(1')–C(2') | -6.46(9) | 4.42(10) | 60.52(8) | 4.82(7) | 48.41(4) |
| **Bond Angles (°)** | | | | | |
| O(2)–Ru–O(3) | 79.16(10) | 78.53(10) | 78.81(8) | 78.10(5) | 78.08(6) |
| O(2)–Ru–Cl | 86.85(7) | 85.59(8) | 84.98(6) | 85.13(4) | 84.77(5) |
| O(3)–Ru–Cl | 83.73(7) | 83.71(8) | 84.80(6) | 84.06(4) | 84.31(5) |

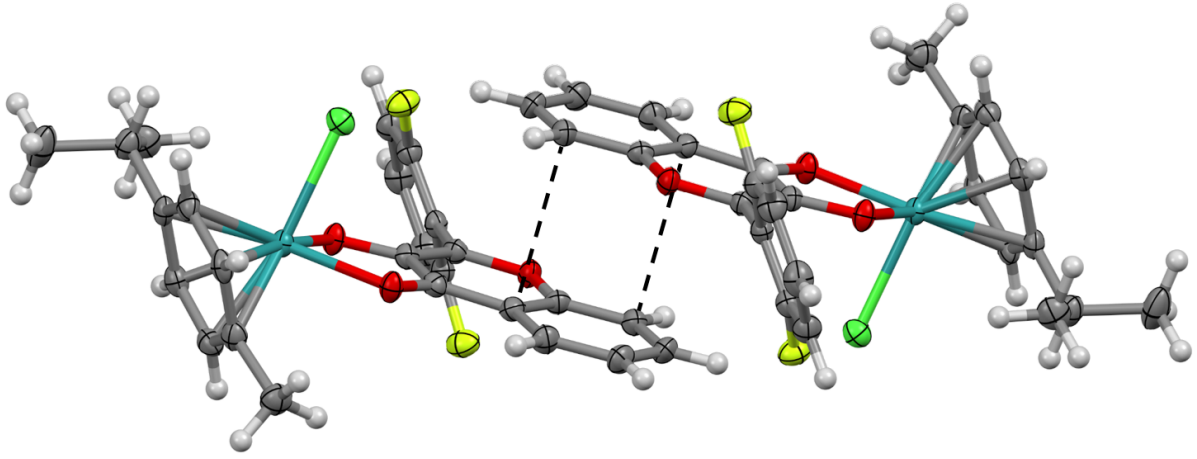

**Figure 3.** π stacking interaction between the planar 3-hydroxyflavone backbones of the two enantiomers of **2d**.

Obviously, this is not a quantitative comparison but rather a relative measure to estimate the compounds' potential to accumulate in cells, which in turn has an impact on the cytotoxicity (Table 4).

**Table 3.** Comparison of the clog*P* values obtained from ChemDraw, Molinspiration and ALOGPS 2.1.

| Compound | clogP | | |
|---|---|---|---|
| | ChemDraw | Molinspiration | ALOGPS 2.1 |
| **1a** | 2.71 | 3.092 | 2.20 |
| **1b** | 3.06 | 3.487 | 2.19 |
| **1c** | 2.35 | 3.077 | 2.08 |
| **1d** | 3.36 | 3.677 | 2.32 |
| **1e** | 3.96 | 4.341 | 3.13 |
| **1f** | 2.09 | 2.664 | 2.04 |
| $\mathbf{A}_{\text{flavone}}$ *a* | 2.35 | 3.609 | 2.38 |

In order to estimate the tumor-inhibiting potential of the ligands **1a–1f** and their complexes **2a–2f**, the cytotoxicity in human ovarian teratocarcinoma [CH1(PA-1)], colon adenocarcinoma (SW480) and non-small cell lung (A549) cancer cells was determined and compared to **A** and the respective HF ligand $\mathbf{A}_{\text{flavone}}$ (Table 4). All complexes, except **2e**, show activity in the low to intermediate μM range and most of them are nearly as active as **A**. With the exception of **1e**, the free ligands are not active in A549 and SW480 cells, but very potent against the ovarian teratocarcinoma CH1(PA-1) cells, which are generally more chemosensitive than the ABC-transporter-overexpressing SW480 and A549 cells. Compound **2e** was not sufficiently soluble to be included in the cytotoxicity assays. This can be explained by the lipophilic nature of its HF ligand **1e**, which however, was the most potent ligand in the *in vitro* anticancer activity assays. The activity of the methoxy-substituted flavones seems to be determined by the position of the OMe groups rather than by the lipophilicity (compare Tables 3 and 4). This is suggested by the fact that **2a** with a methoxy-substituted phenyl ring in positions 3' and 4' is slightly less active than the 3',5'-dimethoxy derivative **2b**. Also, increasing the lipophilicity by addition of a third methoxy group in position 4' led to decreased cytotoxicity. Addition of a second fluoro substituent in *para* position as in **2d** seems to result in even higher $IC_{50}$ values compared with monosubstituted examples [16,17]. In general, the cytotoxicity of these compounds seems to be increased by *ortho* and *meta* substitution, but decreased by introducing halogens in *ortho* position. Considering the data obtained in X-ray diffraction studies, this may be related to the *ortho*-substituent inducing a twist of the phenyl ring around the C(2)–C(1') bond (Figure 2).

**Table 4.** $IC_{50}$ values ± standard deviation for **1a–1e** and **2a–2e** in A549, SW480 and CH1(PA-1) cells with an exposure of 96 h and the experimentally determined solubility in 1%DMSO/medium.

| | Compound | Solubility /μM | $IC_{50}$ / μM | | |
|---|---|---|---|---|---|
| | | 1% DMSO/medium | A549 | SW480 | CH1(PA-1) |
| **methoxy** | **1a** | 330 | > 25 | > 25 | 2.1 ± 0.2 |
| | **2a** | 423 | 18 ± 2 | 8.7 ± 0.8 | 2.2 ± 0.5 |
| | **1b** | 122 | > 25 | > 25 | 1.4 ± 0.2 |
| | **2b** | 358 | 9.0 ± 0.5 | 4.5 ± 0.2 | 1.5 ± 0.2 |
| | **1c** [a] | 111 | > 25 | 8.6 ± 1.5 | 2.0 ± 0.2 |
| | **2c** [a] | 142 | 23 ± 5 | 9.7 ± 1.9 | 2.5 ± 0.3 |
| **fluoro** | **1d** | 92 | > 25 | > 25 | 18 ± 1 |
| | **2d** | 353 | 55 ± 15 | 20 ± 4 | 5.1 ± 0.8 |
| | **1e** | 31 | 6.5 ± 1.5 | 2.6 ± 0.2 | 1.0 ± 0.1 |
| | **2e** | n.s. | – | – | – |
| | $\mathbf{A}_{\text{flavone}}$ [b] | 217 | 7.9 ± 1.2 | 3.7 ± 0.4 | 0.60 ± 0.10 |
| | **A** [b] | 257 | 9.5 ± 0.5 | 3.8 ± 0.5 | 0.86 ± 0.06 |
| **acetamide** | **1f** | 103 | > 25 | > 25 | 7.2 ± 0.3 |
| | **2f** | 187 | 21 ± 1 | 18 ± 1 | 5.3 ± 0.5 |

[a] Values should be taken with caution because precipitation was observed within 24 h at concentrations > 3 μM (**1c**) and > 0.8 μM (**2c**);
[b] taken from ref. [17], n.s. = not sufficiently soluble in 1%DMSO/medium.

# 4 Conclusions

Half-sandwich ruthenium-arene compounds of 3-hydroxyflavones have demonstrated potential in the development as anticancer agents. In order to expand our knowledge about their structure-activity relationships, we have introduced substituents at the phenyl ring of the HF ligand and prepared the respective air and light stable Ru(cym)Cl complexes in good yields. As the lipophilicity is an important parameter in drug development, we calculated the clog*P* values for the 3-hydroxyflavones, and also determined the solubility of the compounds. While the ligands show low aqueous solubility, complexation increases the solubility up to 4-times, with the exception of **2e**. While the stability is not reported for the prepared compounds, the aquation of structurally-related compounds has been reported to be rapid which is, however, not expected to impact behavior in aqueous solution significantly. The cytotoxicity of the new compounds in human ovarian teratocarcinoma [CH1(PA-1)], colon adenocarcinoma (SW480) and non-small cell lung (A549) cancer cells was compared to that of one of the most active compounds in the series so far, *i.e.*, the *p*-fluoro derivative **A**. The compounds inhibited cell proliferation with $IC_{50}$ values in the low μM range but were slightly less active than **A**. Both the ligands and the complexes were particularly potent in CH1(PA-1) cells, while in the other cell lines the complexes were significantly more active than the ligands. There was however, no clear-cut relationship between lipophilicity and cytotoxicity. By analysing the molecular structures of complexes **2b–e** and comparing them to other compounds reported earlier, it appears that the substitution pattern at the phenyl ring has a substantial impact on cytotoxicity. This may be related to twisting of the phenyl ring out of the plane which may cause different interactions with biological targets while factors such as lipophilicity and electronic effects seem to play a minor role.

**Acknowledgements:** We thank the University of Auckland, Genesis Oncology Trust (GOT-1263-RPG), and COST CM1105 for financial support. The authors are grateful to Tanya Groutso for collecting the single crystal X-ray diffraction data and Nick Lloyd for ESI-MS analyses.

# References

[1] Workman, P., Collins, I. Modern Cancer Drug Discovery: Integrating Targets, Technologies, and Treatments for Personalized Medicine. In *Cancer Drug Design and Discovery*, 2nd ed.; Neidle, S., Ed. Academic Press: San Diego, 2014; pp 3-53.

[2] Klein, A.V., Hambley, T.W. Platinum-Based Anticancer Agents. In *Ligand Design in Medicinal Inorganic Chemistry*, John Wiley & Sons, Ltd: 2014; pp 9-45.

[3] Primik, M.F., Filak, L.K., Arion, V.B. Metal-Based Indolobenzazepines and Indoloquinolines: From Moderate CDK Inhibitors to Potential Antitumor Drugs. In *Advances in Organometallic Chemistry and Catalysis*, John Wiley & Sons, Inc.: 2013; pp 605-617.

[4] Oehninger, L., Stefanopoulou, M., Alborzinia, H., Schur, J., Ludewig, S., Namikawa, K., Munoz-Castro, A., Koster, R.W., Baumann, K., Wolfl, S., Sheldrick, W.S., Ott, I., Evaluation of arene ruthenium(II) N-heterocyclic carbene complexes as organometallics interacting with thiol and selenol containing biomolecules, Dalton Trans., 2013; 42, 1657-1666.

[5] Kandioller, W., Balsano, E., Meier, S.M., Jungwirth, U., Goschl, S., Roller, A., Jakupec, M.A., Berger, W., Keppler, B.K., Hartinger, C.G., Organometallic anticancer complexes of lapachol: metal centre-dependent formation of reactive oxygen species and correlation with cytotoxicity, Chem. Commun., 2013; 49, 3348-3350.

[6] Ang, W.H., De Luca, A., Chapuis-Bernasconi, C., Juillerat-Jeanneret, L., Lo Bello, M., Dyson, P.J., Organometallic Ruthenium Inhibitors of Glutathione-S-Transferase P1-1 as Anticancer Drugs, ChemMedChem, 2007; 2, 1799-1806.

[7] Ang, W.H., Parker, L.J., De Luca, A., Juillerat-Jeanneret, L., Morton, C.J., Lo Bello, M., Parker, M.W., Dyson, P.J., Rational Design of an Organometallic Glutathione Transferase Inhibitor, Angew. Chem., Int. Ed. Engl., 2009; 48, 3854-3857.

[8] Hanif, M., Nazarov, A.A., Legin, A., Groessl, M., Arion, V.B., Jakupec, M.A., Tsybin, Y.O., Dyson, P.J., Keppler, B.K., Hartinger, C.G., Maleimide-functionalised organoruthenium anticancer agents and their binding to thiol-containing biomolecules, Chem. Commun., 2012; 48, 1475-1477.

[9] Haquette, P., Salmain, M., Svedlung, K., Martel, A., Rudolf, B., Zakrzewski, J., Cordier, S., Roisnel, T., Fosse, C., Jaouen, G., Cysteine-Specific, Covalent Anchoring of Transition Organometallic Complexes to the Protein Papain from Carica papaya, ChemBioChem, 2007; 8, 224-231.

[10] Tan, Y.Q., Dyson, P.J., Ang, W.H., Acetal-functionalized RAPTA complexes for conjugation and labeling, Organometallics, 2011; 30, 5965-5971.

[11] Babak, M.V., Plażuk, D., Meier, S.M., Arabshahi, H.J., Reynisson, J., Rychlik, B., Błauż, A., Szulc, K., Hanif, M., Strobl, S., Roller, A., Keppler, B.K., Hartinger, C.G., Half-Sandwich Ruthenium(II) Biotin Conjugates as Biological Vectors to Cancer Cells, Chem. Eur. J., 2015; 21, 5110-5117.

[12] Goldbach, R.E., Rodriguez-Garcia, I., van Lenthe, J.H., Siegler, M.A., Bonnet, S., N-Acetylmethionine and Biotin as Photocleavable Protective Groups for Ruthenium Polypyridyl Complexes, Chem. Eur. J., 2011; 17, 9924-9929.

[13] Ang, W.H., Daldini, E., Juillerat-Jeanneret, L., Dyson, P.J., Strategy To Tether Organometallic Ruthenium-Arene Anticancer Compounds to Recombinant Human Serum Albumin, Inorg. Chem., 2007; 46, 9048-9050.

[14] Pagano, N., Wong, E.Y., Breiding, T., Liu, H., Wilbuer, A., Bregman, H., Shen, Q., Diamond, S.L., Meggers, E., From Imide to Lactam Metallo-pyridocarbazoles: Distinct Scaffolds for the Design of Selective Protein Kinase Inhibitors, J. Org. Chem., 2009; 74, 8997-9009.

[15] Nazarov, A.A., Hartinger, C.G., Dyson, P.J., Opening the lid on piano-stool complexes: An account of ruthenium(II)-arene complexes with medicinal applications, J. Organomet. Chem., 2014; 751, 251-260.
[16] Kurzwernhart, A., Kandioller, W., Bachler, S., Bartel, C., Martic, S., Buczkowska, M., Muhlgassner, G., Jakupec, M.A., Kraatz, H.B., Bednarski, P.J., Arion, V.B., Marko, D., Keppler, B.K., Hartinger, C.G., Structure-Activity Relationships of Targeted $Ru^{II}(\eta^6$-p-Cymene) Anticancer Complexes with Flavonol-Derived Ligands, J. Med. Chem., 2012; 55, 10512-10522.
[17] Kurzwernhart, A., Kandioller, W., Bartel, C., Bachler, S., Trondl, R., Muhlgassner, G., Jakupec, M.A., Arion, V.B., Marko, D., Keppler, B.K., Hartinger, C.G., Targeting the DNA-topoisomerase complex in a double-strike approach with a topoisomerase inhibiting moiety and covalent DNA binder, Chem. Commun., 2012; 48, 4839-4841.
[18] Kurzwernhart, A., Kandioller, W., Enyedy, E.A., Novak, M., Jakupec, M.A., Keppler, B.K., Hartinger, C.G., 3-Hydroxyflavones vs. 3-hydroxyquinolinones: structure-activity relationships and stability studies on $Ru^{II}$(arene) anticancer complexes with biologically active ligands, Dalton Trans., 2013; 42, 6193-6202.
[19] Schwarz, M.B., Kurzwernhart, A., Roller, A., Kandioller, W., Keppler, B.K., Hartinger, C.G., Rhodium(Cp*) Compounds with Flavone-derived Ligand Systems: Synthesis and Characterization, Z. Anorg. Allg. Chem., 2013; 639, 1648-1654.
[20] Prajapati, R., Dubey, S.K., Gaur, R., Koiri, R.K., Maurya, B.K., Trigun, S.K., Mishra, L., Structural characterization and cytotoxicity studies of ruthenium(II)–dmso–chloro complexes of chalcone and flavone derivatives, Polyhedron, 2010; 29, 1055-1061.
[21] el Amrani, F.B.-A., Perelló, L., Borrás, J., Torres, L., Development of Novel DNA Cleavage Systems Based on Copper Complexes. Synthesis and Characterisation of Cu(II) Complexes of Hydroxyflavones, Met. Based Drugs, 2000; 7, 365-370.
[22] Dangleterre, L., Cornard, J.-P., Interaction of lead(II) chloride with hydroxyflavones in methanol: A spectroscopic study, Polyhedron, 2005; 24, 1593-1598.
[23] Sathish, S., Narayan, G., Rao, N., Janardhana, C., A Self-Organized Ensemble of Fluorescent 3-Hydroxyflavone-Al(III) Complex as Sensor for Fluoride and Acetate Ions, J. Fluoresc., 2007; 17, 1-5.
[24] Santos, J.P., Zaniquelli, M.E.D., De Giovani, W.F., Galembeck, S.E., Aluminum ion complex formation with 3-hydroxyflavone in Langmuir and Langmuir–Blodgett films, Colloids Surf., A, 2002; 198–200, 569-576.
[25] Lapouge, C., Dangleterre, L., Cornard, J.-P., Spectroscopic and Theoretical Studies of the Zn(II) Chelation with Hydroxyflavones, J. Phys. Chem. A, 2006; 110, 12494-12500.
[26] Nichenametla, S.N., Taruscio, T.G., Barney, D.L., Exon, J.H., A Review of the Effects and Mechanisms of Polyphenolics in Cancer, Crit. Rev. Food Sci, Nutr., 2006; 46, 161-183.
[27] Fotsis, T., Pepper, M.S., Aktas, E., Breit, S., Rasku, S., Adlercreutz, H., Wähälä, K., Montesano, R., Schweigerer, L., Flavonoids, Dietary-derived Inhibitors of Cell Proliferation and in Vitro Angiogenesis, Cancer Res., 1997; 57, 2916-2921.
[28] Harborne, J.B., Williams, C.A., Advances in flavonoid research since 1992, Phytochemistry, 2000; 55, 481-504.
[29] Ross, J.A., Kasum, C.M., Dietary Flavonoids: Bioavailability, Metabolic Effects, and Safety, Annu. Rev. Nutr., 2002; 22, 19.
[30] Cushnie, T.P.T., Lamb, A.J., Antimicrobial activity of flavonoids, Int. J. Antimicrob. Agents, 2005; 26, 343-356.
[31] García-Lafuente, A., Guillamón, E., Villares, A., Rostagno, M., Martínez, J., Flavonoids as anti-inflammatory agents: implications in cancer and cardiovascular disease, Inflamm. Res., 2009; 58, 537-552.
[32] Chen, Z.-T., Chu, H.-L., Chyau, C.-C., Chu, C.-C., Duh, P.-D., Protective effects of sweet orange (*Citrus sinensis*) peel and their bioactive compounds on oxidative stress, Food Chem., 2012; 135, 2119-2127.
[33] Chaudhuri, S., Banerjee, A., Basu, K., Sengupta, B., Sengupta, P.K., Interaction of flavonoids with red blood cell membrane lipids and proteins: Antioxidant and antihemolytic effects, Int. J. Biol. Macromol., 2007; 41, 42-48.
[34] Shen, K.-H., Chen, Z.-T., Duh, P.-D., Cytotoxic Effect of Eucalyptus citriodora Resin on Human Hepatoma HepG2 Cells, Am. J. Chin. Med., 2012; 40, 399-413.
[35] Kandioller, W., Hartinger, C.G., Nazarov, A.A., Kuznetsov, M.L., John, R.O., Bartel, C., Jakupec, M.A., Arion, V.B., Keppler, B.K., From Pyrone to Thiopyrone Ligands–Rendering Maltol-Derived Ruthenium(II)–Arene Complexes That Are Anticancer Active in Vitro, Organometallics, 2009; 28, 4249-4251.
[36] Kandioller, W., Hartinger, C.G., Nazarov, A.A., Bartel, C., Skocic, M., Jakupec, M.A., Arion, V.B., Keppler, B.K., Maltol-derived ruthenium-cymene complexes with tumor inhibiting properties: the impact of ligand-metal bond stability on anticancer activity in vitro, Chem. Eur. J., 2009; 15, 12283-12291.
[37] Kandioller, W., Hartinger, C.G., Nazarov, A.A., Kasser, J., John, R., Jakupec, M.A., Arion, V.B., Dyson, P.J., Keppler, B.K., Tuning the anticancer activity of maltol-derived ruthenium complexes by derivatization of the 3-hydroxy-4-pyrone moiety, J. Organomet. Chem., 2009; 694, 922-929.
[38] Bradley, D., Williams, G., Lawton, M., Drying of Organic Solvents: Quantitative Evaluation of the Efficiency of Several Desiccants, J. Org. Chem., 2010; 75, 8351-8354.
[39] Bennett, M.A., Smith, A.K., Arene ruthenium(II) complexes formed by dehydrogenation of cyclohexadienes with ruthenium(III) trichloride, J. Chem. Soc., Dalton Trans., 1974, 233.
[40] Sheldrick, G.M., A short history of SHELX, Acta Crystallogr., Sect. A: Found. Crystallogr., 2008; A64, 112-122.
[41] Korch, C., Spillman, M.A., Jackson, T.A., Jacobsen, B.M., Murphy, S.K., Lessey, B.A., Jordan, V.C., Bradford, A.P., DNA profiling analysis of endometrial and ovarian cell lines reveals misidentification, redundancy and contamination, Gynecol. Oncol., 2012; 127, 241-248.
[42] Tetko, I.V., Gasteiger, J., Todeschini, R., Mauri, A., Livingstone, D., Ertl, P., Palyulin, V.A., Radchenko, E.V., Zefirov, N.S., Makarenko, A.S., Tanchuk, V.Y., Prokopenko, V.V., Virtual computational chemistry laboratory--design and description, J. Comput. Aided Mol. Des., 2005; 19, 453-463.
[43] Bennett, M., Burke, A.J., O'Sullivan, W.I., Aspects of the Algar-Flynn-Oyamada (AFO) reaction, Tetrahedron, 1996; 52, 7163-7178.